HAL
archives-ouvertes.fr

Risk assessment of a fire involving combustible materials in a warehouse

H.Y. Wang, P. Russo, P. Joulain, André Carrau

▶ To cite this version:

H.Y. Wang, P. Russo, P. Joulain, André Carrau. Risk assessment of a fire involving combustible materials in a warehouse. BRADLEY, D. ; DRYSDALE, D. ; MOLKOV, V. 4. International seminar on fire and explosion hazards, Sep 2003, Londonderry, Ireland. pp.523-534, 2004. <ineris-00972482>

HAL Id: ineris-00972482
https://hal-ineris.archives-ouvertes.fr/ineris-00972482

Submitted on 3 Apr 2014

HAL is a multi-disciplinary open access archive for the deposit and dissemination of scientific research documents, whether they are published or not. The documents may come from teaching and research institutions in France or abroad, or from public or private research centers.

L'archive ouverte pluridisciplinaire **HAL**, est destinée au dépôt et à la diffusion de documents scientifiques de niveau recherche, publiés ou non, émanant des établissements d'enseignement et de recherche français ou étrangers, des laboratoires publics ou privés.

RISK ASSESSMENT OF A FIRE INVOLVING COMBUSTIBLE MATERIALS IN A WAREHOUSE

Wang, H.Y. [1], Russo, P. [1,2], Joulain, P. [1] and Carrau, A. [2]

[1] Laboratoire de Combustion et de Détonique, CNRS, ENSMA, **Université de Poitiers, BP 109, 86960, Futuroscope Cedex, France**

[2] Institut National de l'Environnement Industriel et des Risques (INERIS), Verneuil-en-Halatte, France

ABSTRACT

This paper presents the results of a numerical modeling into a rack fire in warehouse, and an identification of the visible flame shape when a fire is generalized over a whole warehouse after collapse of the roof. The model described here is a numerical implementation of a thermal and fluid-dynamic theory to predict the rate of flame spread. Evolution of the thermodynamic system is governed by the conservation equations for total mass, momentum (Navier-Stokes), energy and species mass fractions. Large-Eddy-Simulation method is used in which the large-scale eddies that govern the mixing of the gases are directly simulated. The sub-grid scale motion is calculated using the Smagorinsky model. The combustion process is assumed to be controlled by diffusion, permitting a mixture-fraction-based modeling approach The radiant flux vector in the energy equation is calculated by integrating the radiation intensity over all directions. The radiation intensity is found by solving a radiative transfer equation without scattering. A one-dimensional heat conduction equation for the condensed phase temperature is applied. The mass loss rate of volatiles from the solid fuel surface is assumed to obey the simple Arrhenius equation. At first, the work was focused to a fully coupled solution for a single rack fire configuration to both the fluid dynamics and radiative transport equations. The prediction for a single rack fire configuration is in good agreement with the experimental data. Then, the numerical model is extended to the determination of the flame height of a warehouse fire for comparison with the available correlations. It is found that the warehouse fire looks like a cone of flame with a rectangular base.

NOMENCLATURE

A	frequency factor (kg/m^2 s)	Sf	flame surface (m^2)
c_p	specific heat (J/kg K)	S_{ij}	local large scale rate of strain (1/s)
C_s	Smagorinsky constant	T	temperature (K)
D_{eq}	equivalent diameter (m)	T_∞	ambient temperature (K)
E	activation energy (J/mol)	u	velocity vector (m/s)
g	acceleration of gravity (m/s^2)	w	horizontal spacing between solid fuel
h	enthalpy (J/kg)	W	warehouse width (m)
H	total rack height (m)	z	vertical co-ordinate
H_f	flame height (m)	z_0	virtual source location (m)
I	radiation intensity (W/m^2 sr)	Z	mixture fraction
L	warehouse length (m)	p	density (kg/m^3)
m_s	mass loss rate (kg/m^2 s)	ρ_∞	ambient density (kg/m^3)
p	pressure (Pa)	μ_t	eddy viscosity (kg/m s)
Pr_t	turbulent Prandtl number	K	absorption coefficient (1/m)
$\dot{q}_c'''$	heat release rate per unit volume	A	length scale (m)
q_r	radiant flux vector (W/m^2)	α, β, a, b	: correlation parameters
Q	total heat release rate	k, c, η:	correlation parameters
Q_c	convective heat release rate	χ_c	combustion efficiency

Sc_t turbulent Schmidt number χ_r radiative fraction

τ_{ij} Reynolds stresses

INTRODUCTION

Warehouse fires are potentially serious. Warehouse fires are usually limited in size but behave as intense emitters of heat, smoke and other combustion products. In the warehousing field, fire safety is fundamental for the protection of human beings and the environment. In this paper, a methodology for simulating a spread fire along the solid surface in rack configuration is presented. This aspect has always occupied a large proportion of the research effort [1-4] in fire science. Assessing the hazard of combustible materials requires an understanding of the effect of such geometries on flame height and temperature/ velocity fields. However, in the task for obtaining the experimental data or analytical solution for a large-scale warehouse fire, it is not possible to describe the flame-surface heat flux. Therefore, as a first step towards describing fire propagation in rack storage configuration, this paper presents an application of Large-Eddy-Simulation (LES) for solving the thermal and fluid-dynamic equations of 3D elliptic, reacting flow. For this, the Fire Dynamics Simulator (FDS) code, developed by NIST [5], is used. The numerical model is validated against the experimental data obtained by Ingason [1-3] for a single rack fire, and a good agreement is observed.

However, it is now relatively expensive to perform a CFD calculation in the design phase for safety consideration of a warehouse. Therefore, engineering methods have become important in the development of tools to assist in the design procedure. However, in the case of warehouses, fire safety engineering techniques arc less developed [6], there is no method available which reveals whether the design is sufficiently safe and economic. As a fire is generalized over a whole warehouse after collapse of the roof, the flame height becomes the most important parameter. Because near the fire, over a distance comparable to the flame height, the radiant energy flux can be sufficiently high to threaten both the structual integrity of neighbouring buildings, and the physical safety of firefighters and personnel. According to McCaffrey [7-8], the flame can be divided into three regions: the continuous flame region, the intermittent region, and the smoke plume. In his work, various correlations have been developed for the evaluation of thc velocities and temperatures in the plume zone. Many analytical studies [9-13] about the pool-like fire of cellulose products or hydrocarbons in a laboratory scale have been also conducted to establish the mean flame height corrclations. Heskestad [4] made some modifications to his original correlation for adapting a rack fire configuration. In particular, Ingason [1-3] has undertaken a theoretical and experimental study about the fires in rack storage. He introduced various correlations on the heat release rate, the flame height and the in-rack centreline temperaturc/ velocity. Large-scale fires (D>20 m) have also been studied by Koseki [14], and the maximum of the radiation intensity emitted by the large-scale flame was found to vary between 10 and 90 kW/m^2 depending on the fuel properties. The second part of this numerical study aims at evaluating and improving engineering tools for use in warehouse fire safety. The first task of this work is to evaluate the capability of the current flame height correlations to analyse the warehouse fire hazard. It is found that some correlations for flame hcight are often used apart from the domain of validity for the study of a warehouse fire, in particular for the line type warehouse configuration.

THEORETICAL ANALYSIS

In this work, Large Eddy Simulation (LES) is used to solve the gas phase model, which consists of the conservation equations for mass, momentum (Navier-Stokes), and encrgy

$$\frac{\partial \rho}{\partial t} + \mathrm{V}.\rho \mathrm{u} = 0, \tag{1}$$

$$\rho\left(\frac{\partial \mathbf{u}}{\partial t} + (\mathbf{u}\cdot\nabla)\mathbf{u}\right) = -\nabla p + \rho\mathbf{g} + \nabla\cdot\tau_{ij,SGS}, \tag{2}$$

$$\frac{\partial \rho h}{\partial T} + \nabla \cdot \rho \mathbf{u} h = \frac{Dp}{Dt} + \dot{q}_c''' + \nabla \cdot (\mu_t / \mathrm{Pr}_t) \nabla h - \nabla \cdot \mathbf{q}_r . \quad (3)$$

The basic idea behind LES is that the eddies, accounting for most of the mixing, are large enough to be calculated with reasonable accuracy from the equations of fluid dynamics. The sub-grid scale motion is calculated by use of the Smagorinsky model [5] which relates the unknown subgrid scale (SGS) Reynolds stresses, $\tau_{ij,SGS}$, to the local large scale rate of strain

$$\tau_{ij,SGS} - \frac{1}{3}\tau_{kk,SGS}\delta_{ij} = 2\mu_t S_{ij} \quad \text{with} \quad S_{ij} = \frac{1}{2}\left(\frac{\partial u_i}{\partial x_j} + \frac{\partial u_j}{\partial x_i}\right). \quad (4)$$

The eddy viscosity is based on the local length scale, Δ, and time scale, S_{ij},

$$\mu_t = C_s^2 \rho \Delta^2 |S_{ij}| \quad \text{with} \quad C_s \approx 0.21 . \quad (5)$$

Combustion process is assumed to be controlled by diffusion, permitting a mixture-fraction-based modelling approach

$$\frac{\partial \rho Z}{\partial t} + \nabla \cdot (\rho Z)\mathbf{u} = \nabla \cdot (\mu_t / Sc_t) \nabla Z . \quad (6)$$

The oxygen mass conservation equation can be transformed into an expression for the local heat rate using the conservation equation (6) for the mixture fraction and a state relation [5].

The radiant flux vector in the energy equation is calculated as follows

$$-\nabla \cdot \mathbf{q}_r = \kappa(\mathbf{x})[U(\mathbf{x}) - 4\pi I_b(\mathbf{x})] \quad \text{with} \quad U(\mathbf{x}) = \int_{4\pi} \mathrm{I}(\mathbf{x},\mathbf{s}) d\Omega . \quad (7)$$

Here, the radiation intensity is obtained by solving the radiative transfer equation without scattering

$$\vec{\nabla} . \vec{\Omega} I + \kappa I = \kappa \frac{\sigma T^4}{\pi} . \quad (8)$$

In the condensed phase, a one-dimensional heat conduction equation is solved. The mass loss rate, $\dot{m}_s$, of volatiles from the surface is assumed to obey the simple Arrhenius expression, $\dot{m}_s = A e^{-E/RT}$ ($\mathrm{kg/m^2 s}$). The frequency factor, A, and the activation energy, E/R, are taken as 2.6 10^8 and 12000 (K), respectively for this paper carton. The ignition temperature is given as 250 °C. The finite-difference technique is used to discretize the partial differential equations and the associated boundary conditions. All the spatial derivatives are approximated by a second-order central differences scheme and the flow variables are updated in time using an explicit second-order Runge-Kutta scheme [5].

VALIDATION OF THE NUMERICAL MODELS

At first, the prediction is compared with the experimental data in the rack fire configuration in terms of heat release rate, flame height, temperature and velocity. The schematic diagram of the rack storage arrays examined experimentally by Ingason [1-3], and the coordinate system adapted from his work in numerical simulation are shown in Figure 1.

In the experiment of Ingason [1-3], a Standard Class II storage commodity [6] which consists of double triwall corrugated paper cartons was used. The outer dimensions of each carton were 1.2 m (x) x 0.8 m (y) x 1.0 m (z). The total height of the rack storage was 5.2 m and had four tiers. Four ignition

sources were symmetrically placed close to the centre of the storage arrays at the bottom of each carton of the lowest tier. The mean temperature and gas velocity were measured at four elevations, z=0.97, 2.27, 3.57 and 4.87 m. The horizontal spacing (cf. Fig. 1), w, between the cartons varied from 75, 150, 225 to 300 mm. In the numerical study, a rather similar fire condition was used. The ignition sources were simulated by four burners with a heat release of 30 kW each during 30 seconds. The complex characteristics of carton paper were taken as those of wood. A typical grid contains about 576000 cells (48 x 48 x 250), and the calculation required about 15 x 24 h on HP4000 workstation for 4 minutes simulation of the events.

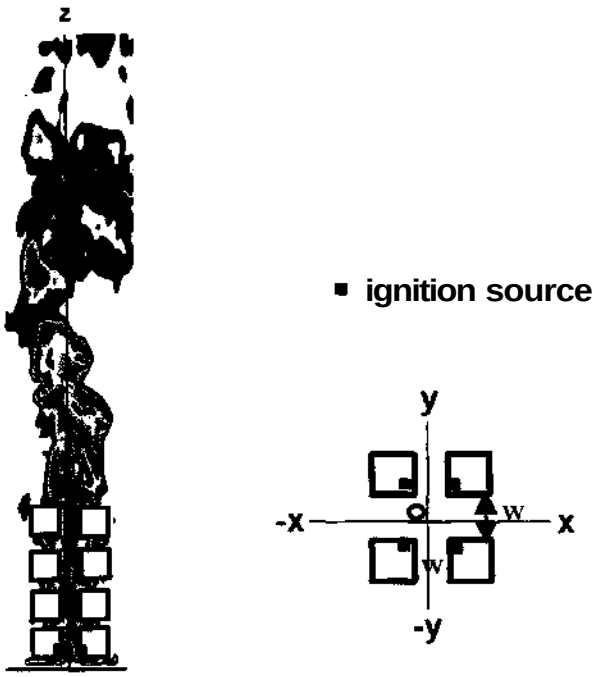

Figure 1. Instantaneous snapshot of a rack fire, and the coordinate system in numerical simulation.

The evolution of the rates of heat release determined in experiments [1-3] and predicted by use of the numerical model as a function of the horizontal spacing, w, is shown in Figure 2. From the experimental data for $Q \leq 10$ MW, Ingason [1-3] proposes the following relation to describe the rate of heat release:

$$Q_c = H\alpha e^{\beta t}(a + bt). \qquad (9)$$

The parameters α, β, a, b can be determined from experimental data. This correlation is a combination of the exponential and power law variations. The fire spread can be divided [1-3] into three periods : the incipient period, the fast upward fire spread period and the horizontal fire spread period. In the second period, the fire growth along the vertical channels between adjacent stacks is rather faster than that in the incubation period. However, the third is the most hazardous period. A similar trend between the prediction and experiment as a function of the horizontal spacing, w, is observed. In the experiment, during the horizontal fire spread period, the slope of the curve of the heat release rate increases with the increase of the horizontal spacing, w. However, the numerical model does not correctly predict this trend, and the predicted incubation and take-off periods are shorter as compared to the experimental ones. We believe that the main reasons for this divergence are bound to the assumption taken for carton properties and for the simulation of the operation of the ignition source. Moreover, in the experiment, the paper cartons disappear progressively due to burning. This burning away condition is not taken into account in the numerical simulation, resulting in a big difference for the evolution of the heat release rate between prediction and experiment.

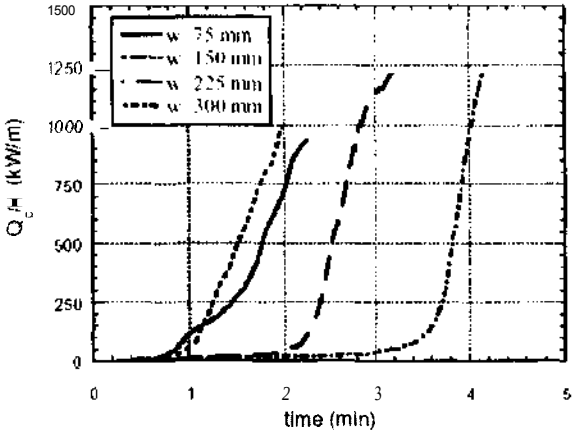

(a) Experimental data

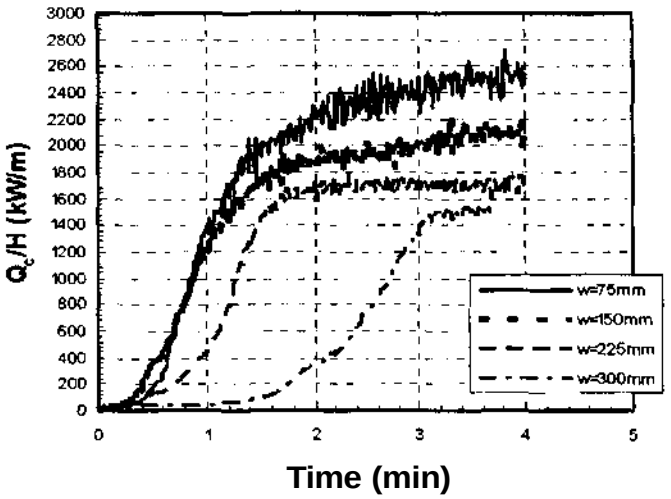

(b) Numerical results

Figure 2. Evolution of the convective heat release rate normalized by the height of the rack storage as function of the time for different horizontal spacing, w.

A comparison between the predicted flame height and experimental data as a function of $Q^{2/5}$, is plotted in Figure 3 for different horizontal spacing, w. For the prediction, the mean flame height corresponds to the zone where the temperature is higher than 500°C during one second. The experimental data suggests the following correlation for the flame height:

$$H_f = -3.73\, w + 0.343 Q^{2/5} \tag{10}$$

which is valid only for $L \leq H$. For $Q^{2/5}/w<50(\mathrm{kW}^{2/5}/\mathrm{m})$, the predicted flame height as a function of the heat release rate, $Q^{2/5}$, follows closely the correlation (10). However, for $Q^{2/5}/w>50\ (\mathrm{kW}^{2/5}/\mathrm{m})$, the slope of the predicted flame height is steeper than that obtained by the correlation. The flame height for the smallest horizontal spacing, w=75 mm, takes a different form compared to the three others. It is probably due to influence of the burners because the flame reaches the top of the rack while the burners are operational for w=75 mm. In general, the flame spread velocity increases when the horizontal spacing, w, decreases.

Following the Ingason analysis [1-3], an analytical relation for the in-rack excess centreline temperature, ΔT, is established as a function of the convective heat release rate, as:

$$\Delta T = 28\left[\frac{T_\infty}{g c_p^{\,2} \rho_\infty^{\,2}}\right]^{1/3} \frac{Q_c^{\,2/3}}{(z - z_0)^{5/3}}, \tag{11}$$

where z_0 is the virtual source location, defined as:

$$z_0 = -3.73w + 0.0083Q^{2/5}. \tag{12}$$

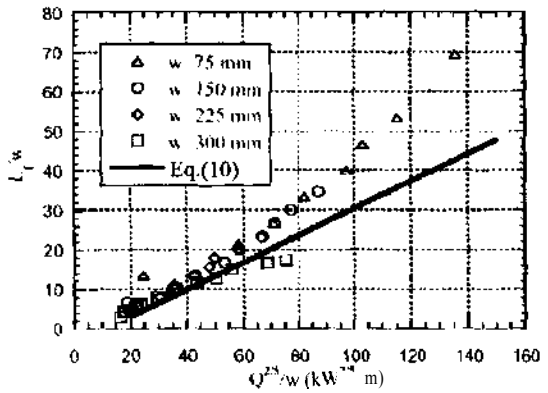

(a) Experimental data against correlation [1-3]

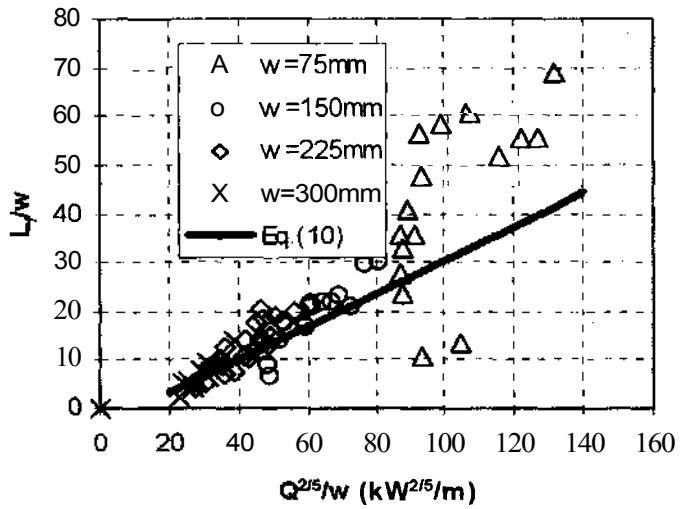

(b) Numerical results against correlation [1-3]

Figure 3. Evolution of the non-dimensional flame height as a function of the heat release rate parameter, $Q^{2/5}$ for different horizontal spacing.

A comparison between the predicted and measured temperature along the rack excess centreline as a function of the convective heat release rate is plotted in Figure 4 for three elevations, z=2.27, 3.57 and 4.87 m. Globally, the evolution of the excess centreline temperature is consistent with a large body of the experimental data and the correlation (1 1). For $(z-z_0)/Q_c^{2/5}>0.2$ m/kW$^{2/5}$, the temperature increases following the power -5/3 of the abscissa. It should be noted that, at the base of the rack fire (z<1.0 m), the temperature is practically independent of the heat release rate. Therefore, the correlation (11) is found to be valid only far away from the base of the rack.

An analytical relation of the gas velocity along the rack centreline is also established according to Ingason's experimental data [1-3] as a function of the convective heat release rate, as:

$$u = 3.54\left[\frac{g}{c_p \rho_\infty T_\infty}\right]^{\frac{1}{3}}\left(\frac{Q_c}{z - z_0}\right)^{0.45} \tag{13}$$

A comparison between the predicted and measured gas velocity along the rack centreline as a function of the convective heat release rate is presented in Figure 5 at three elevations, z=2.27, 3.57 and 4.87 m. The numerical model tends to underestimate the centreline velocity, and however, produce a similar trend as compared to the experimental one. In general, the centreline velocity increases as the horizontal spacing, w, decreases. As for the centreline temperature, the correlation (13) is not valid at the base of the rack fire (z<1.0 m).

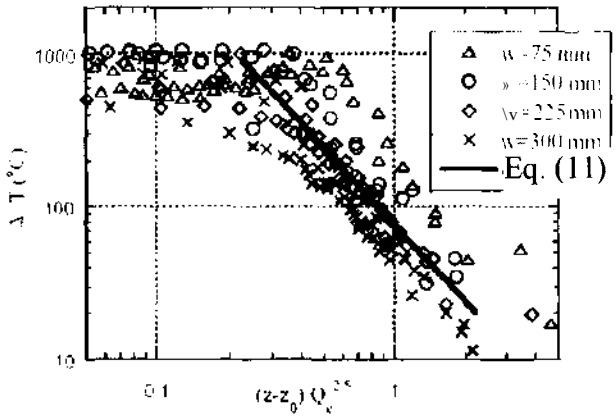

(a) Experimental data against correlation [1-3]

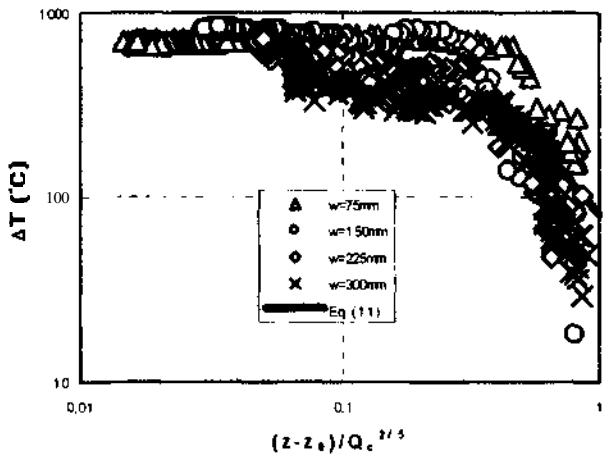

(b) Numerical results against correlation [1-3]

Figure 4. Evolution of the excess centreline temperature as a function of the convective heat release rate for different horizontal spacing, w, at z =2.27, 3.57 and 4.87m.

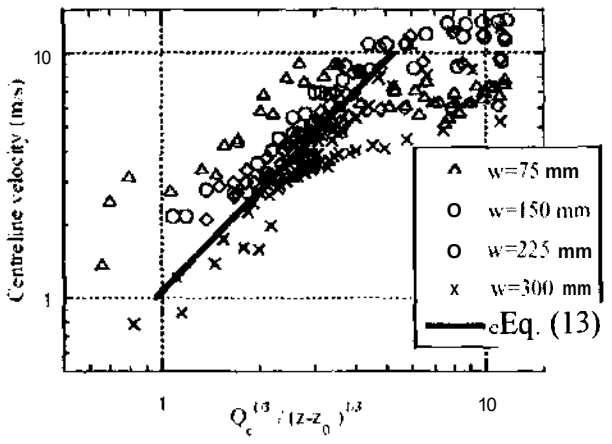

(a) Experimental data against correlation [1-3]

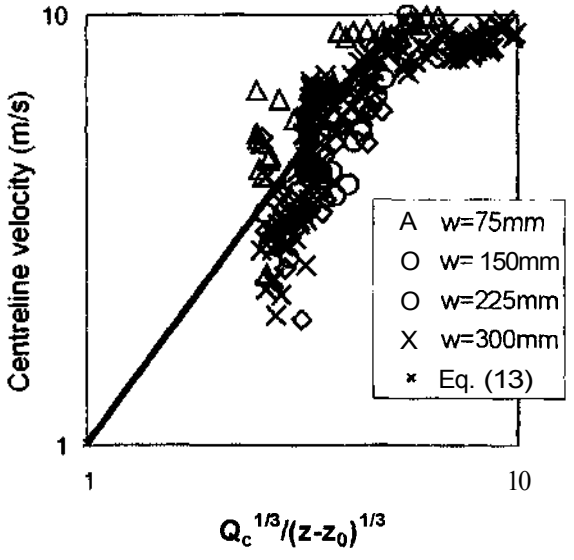

(b) Numerical results against correlation [1-3]

Figure 5. Evolution of the centreline gas velocity as a function of the convective heat release rate for different horizontal spacing, w, at z =2.27, 3.57 and 4.87 m.

FIRE GENERALIZED OVER A WHOLE WAREHOUSE

It can be seen that in a warehouse with rack storage, the flame reaches rapidly the ceiling as the fire growth rate becomes extremely important. Both quantity and type of combustible materials, once ignited, play a major role on the flame height and on the emission of toxic chemical species. However, the complexity of the problem is such that a full simulation of the scenario including a fire spread in the incipient period, and a potential post-flashover fire encompassing realistic, arbitrary conditions in a large-scale warehouse remains intractable. So far, fire safety design has been highly reliant on prescriptive rules in warehouse codes which specify the maximum allowed distance to a fire exposed personnel. In fact, as the time elapses, collapse of the roof (usually steel) may occur due to heat transfer to the structure from the fire. So, in this study, the foreseeable worst-case scenario has been chosen with the following features: 1) a fire is generalized over a whole warehouse with a surface of 7500 m^2; 2)

presence of a large number of racks with a height of 10 m in the warehouse; 3) all the surfaces of the solid or liquid materials are burning with a mean mass loss rate of about 7 g/m^{2}s. This value of mass loss rate is provided by FDS [5] Database file for a large rack fire of plastic products. A schematic diagram of the rack disposition in the horizontal plane of a warehouse, and the coordinate system in the numerical simulation are illustrated in Figure 6. Two warehouse configurations, differing each other by the length to width ratio, L/W, are considered. The length (L) and width (W) of the warehouse are respectively set to 150 m and 75 m for L/W=2, and 250 m and 30 m for L/W=8 with a warehouse height of 13 m. The symmetry conditions are used in the computation model. Figures 7-8 show a schematic representation of a warehouse fire from a computation of the reacting fluid dynamics with about 600000 grid cells.

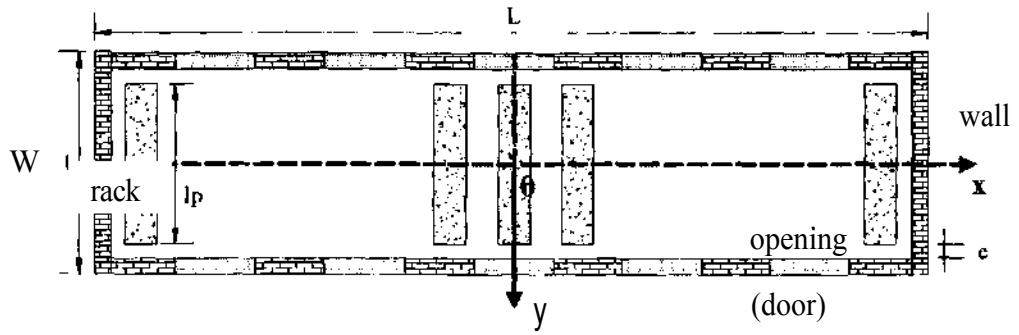

Figure 6. Schematic diagram of the rack disposition in the horizontal plane of a warehouse, and the coordinate system in numerical simulation

According to the numerical study (cf. Figs. 7-8), the visible flame shape of a warehouse fire where the temperature is higher than 500 °C looks like a cone with a rectangular base. For the sides perpendicular to racks, the flame shape can be treated as a fire wall with a surface of $L_{ob} \times L$ m^2 where L_{ob} is the oblique side of the cone (cf. Fig. 8), given as:

$$L_{ob} = \sqrt{(0.5 \times W)^2 + H_f^2}, \text{ (m)}. \tag{14}$$

For the sides parallel to racks, the flame shape can be taken as a triangular fire wall with a surface of 0.5 x HfX W m^2. The volume of the cone with a rectangular base can be obtained as:

$$V_{cone} = 0.5W \times (H_f - H) \times L, \quad (\text{m}^3). \tag{15}$$

In Eq.(15), the warehouse walls are accounted for by blocking portions of the radiation through the reduction in the cone volume (configuration factor). However, for the worst-case scenario, the warehouse walls should not be taken into account (H=0). The radiation intensity from flame is obtained by

$$\phi_0 = \frac{\chi_r \chi_c \dot{Q}_c}{S_f}, \quad (\text{kW/m}^2) \tag{16}$$

For the large-scale warehouse fire, the combustion process is controlled by the air entrainment. Based on the oxygen consumption from FDS simulation, the maximum effective heat release generated by a warehouse fire with a burning surface (racks) of 60000 m^2 for L/W=2 can reach 3000 MW for a solid material (PMMA), and 5000 MW for an hydrocarbon fuel (heptane). So, the effective heat release accounts for about 30 percent of the theoretical total heat release, $\dot{Q}_c$ (that is, combustion efficiency $\chi_c = 0.3$). In general, the radiative fraction, χ_r, is assumed to be 0.35 for a large-scale fire. For L/W=2, the warehouse fire can be simulated by a cylindrical pool-like fire with an equivalent diameter obtained from

$$D_{eq} = \sqrt{4V_{cone}/(\pi H_f)}, \quad (\mathrm{m}). \tag{17}$$

The equivalent flame surface is calculated by

$$S_f = 0.5\pi D_{eq}^2 + \pi D_{eq} H_f, \quad (\mathrm{m}^2). \tag{18}$$

However, for L/W=8, the cone with a rectangular base, as shown in Figures 7-8, should be applied for the calculation of the view factors (F). The flame surface corresponding to the cone is

$$S_f = 2L_{ob}L + LW + WH_f, (\mathrm{m}^2). \tag{19}$$

A comparison between the predicted flame height and the correlations for L/W=2 with an equivalent diameter of 82 m (Eq.17) is presented in Figure 9. Among relationships for the flame height which have been proposed, McCaffrey's correlation [8] for the particular purpose of warehouse fire applications appears the most suitable to fit the prediction from the FDS simulation. This flame height correlation is derived from the temperature one as

$$H_f = Q^{2/5}\left(\frac{2g}{K'} \times \frac{T_f - T_0}{T_0}\right)^{\frac{1}{2\eta-1}}, \quad (\mathrm{m}). \tag{20}$$

Here, K' is defined as $K' = (k/c)^2$.The following values in Eq.(20), T_f= 773 K, T_0 =300 K, k=1.9, c=0.9 and $77 = 0$, are used for calculating the flame height. However, all the other flame height correlations [10-13] based on a fire diameter give results far away from the predicted flame height. It should be noted that, for a warehouse fire with the presence of a large number of racks, it is difficult to determine an equivalent diameter. Particularly, for a large-scale fire with an equivalent diameter of 82 m, the flame height correlations [10-11] are completely out of its intended range of validity. Based on the flame height to which the radiant energy emitted by flame is directly proportional, the radiation intensity calculated from Eq.(16) is presented in Table I for the different products.

INERIS has developed an analytical software, FNAP [15], which can be used for determining the safety areas around a warehouse in fire where humans will bear radiation levels emitted from a flame to 3 kW/m^2 for unprotected people or to 5 kW/m^2 for protected fire-fighters. In order to obtain the local heat flux from this code, some parameters, such as radiation intensity (ϕ_0) from flame, transmission in air (τ) and adds the relevant view factors (F),should be specified

$$\phi = \phi_0 F \tau, \quad (\mathrm{kW/m^2}). \tag{21}$$

Based on the type of combustible materials, the flame height, H_f, from McCaffrey's correlation (20), the radiation intensity, ϕ_0, from Table I, and the view factors, F, from a cone configuration Eq.(15) can be determined.

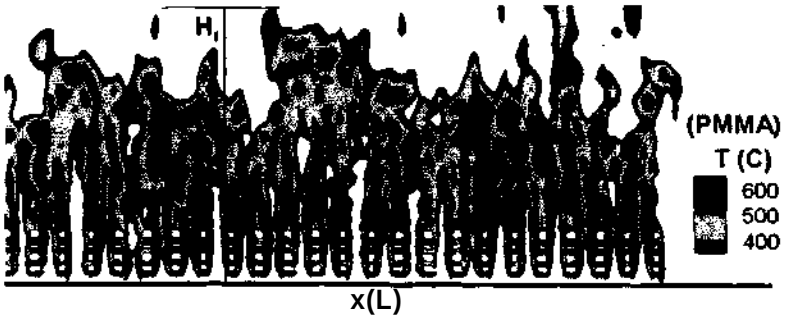

Figure 7. Temperature contours on the median plane perpendicular to racks.

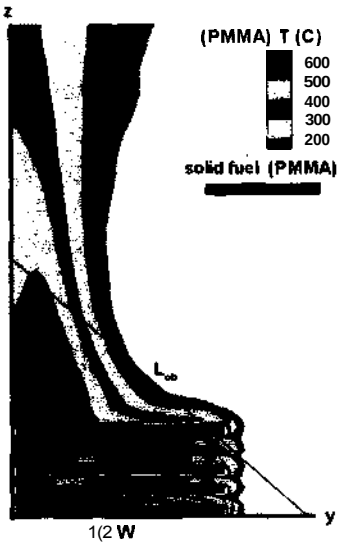

Figure 8. Temperature contours in a cross-section parallel to racks.

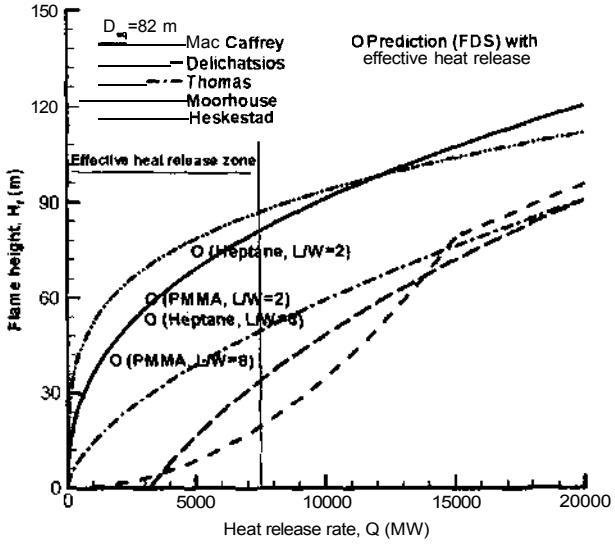

Figure 9. Comparison of flame heights between correlations and predictions for PMMA and heptane.

ϕ_0, kW/m^2	Hydrocarbon products	Plastic products	Cellulosic products	Feeding products
L/W=2	68	41	36	23
L/W=8	45	26	22	15

Table 1. Radiant energy intensity emitted by flame for four different products.

CONCLUSION

Globally, the predicted results for a single rack fire are found in good agreement with the experimental data [1-3], and follow approximately the correlation trend. According to this numerical study, the flame spread is found rather fast along the solid fuel in rack storage due to chimney effects. For the rack fire, the contribution of radiation to the flame spread is dominant. As a fire is generalized over a whole warehouse after collapse of the roof, the visible flame height is about 3 times the rack (in burning) height for *L/W*=8, and however, 7 times the rack height for *L/W*=2. As compared to the numerical results, McCaffrey correlation (20) can be used to determine the visible flame height for a warehouse fire.

However, there are still lacks in the understanding of how a rack fire is evolved spatially and temporally in an enclosure where the ventilation is rather limited. The results as presented here cannot yet be regarded as complete. It can therefore be stated, that despite the relatively simple analytical solution available today, to meet fire safety design requirement, the procedure still lack of flexibility in their use may lead to unnecessarily expensive warehouse. It would be highly desirable to relate the burning rate to the total heat flux from the flame to the fuel surface for a large-scale fire. Also, future development should relate the soot generation rate to the local oxygen and temperature fields for determining the real radiation fraction.

REFERENCES

1. Ingason, H., Experimental and Theoretical Study of Rack Storage Fires, Lund University, Sweden Institute of Technology Department of Fire Safety Engineering, 1996.

2. Ingason, H., Heat Release Rate of Rack Storage Fires, SP Swedish National Testing and Research Institute, 2001.
3. Ingason, H., An Experimental Study of Rack Storage Fires, Brandforsk Project 602-971, Report 19, 2001.
4. Heskestad, G., Flame Heights of Fuel Arrays with Combustion in Depth, Proceedings of the 5th International Symposium on Fire safety Science, 1997, pp. 427-438.
5. McGrattan, K. B., Glenn, P.F. and Jason, E.F., Fire Dynamics Simulator, Technical Reference Guide, NIST Technical Report, 2000.
6. Technical Reports, ISOTR 13387, Fire Safety Engineering, 1999, Parts 1-8.
7. McCaffrey, B.J., Purely Buoyant Diffusion Flames: Some Experimental Results, NBSIR 79-1910, National Bureau of Standards, 1979.
8. McCaffrey, B.J., Flame Height, SFPE Handbook of Fire Protection Engineering, 2nd ed., National Fire Protection Association, Quincy, MA, 1995, pp. 21-28.
9. Zukoski, Cetegen and Kubota, Visible Structure of Buoyant Diffusion Flames, 20th International Symposium on Combustion, The Combustion Institute, 1984, pp. 361-366.
10. Heskestad, G., Engineering Relations for Fire Plumes, *Fire Safety Journal,* 7, 1984, pp. 25-32.
11. Delichatsios, M.A., Air Entrainment into Buoyant Jet Flames and Pool Fires, *Combustion and Flame*, 70, 1987, pp. 33-46.
12. Thomas, P.H., The Size of Natural Fires, 9th International Symposium on Combustion, The Combustion Institute, 1963, pp. 844-859.
13. Moorhouse, Scaling Criteria for Pool Fires Derived from Large-Scale Experiments, Int. Chem. Sym., 1982.
14. Koseki, H., Large Scale Pool Fires : Results of Recent Experiments, Proceedings of the 6th International Symposium on Fire safety Science, 1999, pp. 115-132.
15. INERIS, Feux de Nappe, 2002, www.ineris.fr